

Computational Study on Structural Behaviour of Cold-Formed Steel Built-Up I-Section Beams

Nur Azrinna Sari¹, Koh Heng Boon^{2*}

^{1,2}Faculty of Civil Engineering and Built Environment,
Universiti Tun Hussein Onn Malaysia, Batu Pahat, 86400, MALAYSIA

*Senior Lecturer, Faculty of Civil Engineering and Built Environment, Universiti Tun Hussein Onn Malaysia

DOI: <https://doi.org/10.30880/rtcebe.2023.04.03.045>

Received 06 January 2022; Accepted 15 May 2023; Available online 31 December 2023

Abstract: Cold-formed steels are usually applied in pairs to achieve increased moment stability and bearing performance. This paper presents the finite element analysis (FEA) on buckling behavior of cold-formed steel built-up I-section beams. The I-beams were built up using back-to-back cold-formed plain channel sections. Two series of beams with single and double rows of bolts with 5 different end restraints were modeled using LUSAS FEA software. The plain channels were modelled as 3D surface elements and the bolts were assigned as joint with rotational stiffness. The beams were subjected to 4-point bending and buckling analysis were carried out to determine the buckling mode and the capacity. From the FEA, single and double rows of cold-formed built-up I-section beams performed almost the same buckling behavior. The beams with the supports of lateral end restraint (translation in z) and fully fixed had shown significant increment of the buckling capacity compared with beams with simply supported. Overall, end restraint plays an important role in the cold formed built-up beams.

Keywords: Built-Up I-Beams, Buckling Load, FEA

1. Introduction

Cold-formed steels are usually applied in pairs to achieve increased moment stability and bearing performance. As a result, back-to-back built-up channel beams are increasingly being used in cold-formed steel (CFS) constructions. I-beams are frequently produced from two C-sections back-to-back in cold-formed steel construction using two rows of connectors near both flanges [1]. Screws, bolts, clinches, and spot welds are common connectors [2]. Hence, cold-formed steel members are also thinner, lighter, and easier to manufacture, as well as being less expensive than hot-rolled steel members. The lightweight CFS structural elements can give a higher strength-to-weight ratio, more variable member profiles, and also ease onsite fabrication and installation [3]. Moreover, the most frequently encountered mechanisms of structural instability failure for CFS members are lateral torsional buckling (LTB), flexural buckling (FB), flexural torsional buckling (FTB), and interactive buckling (local and distortional buckling with LTB and FTB) [4]. Additionally, the finite-element method (FEM), also known as finite-element analysis (FEA), is a useful computational technique for

*Corresponding author: koh@uthm.edu.my

2021 UTHM Publisher. All rights reserved.

publisher.uthm.edu.my/periodicals/index.php/rtcebe

estimating solutions to complex structural mechanical problem [5]. Finite element analysis (FEA) is a powerful tool for exploring the failure mechanism and predicting the ultimate strength of cold-formed steel structural components due to its high efficiency and low cost [6].

Therefore, this project aims to study the structural behavior of cold-formed steel built-up I section beams by using finite element analysis which is LUSAS Software. Cold-formed channel sections are used to form up I-section beams with different arrangement and position of bolts at the web of channels and the difference of end-support toward the beams. Hence, computational study by finite element analysis software is used to model and predict the buckling capacity of the built-up I-section cold formed steel beams.

2. Methodology

The methodology used in this project consists of the validation of the FEA model for control beam, parametric study for cold-formed steel beams for single and double rows of bolts with different end-restraint, and the process of finite element modelling of cold-formed steel built-up I-section beam.

2.1 Validation of FEA Model for Control Beam

The validation of finite element analysis has been implemented to compare the results between the finite element analysis, theoretical calculation, and previous finite element study by Wong (2006). The beam is designed of cold- formed steel I-beam using back-to-back lipped channel and connected by 12 mm size of bolted connection. The dimension and properties of the beam are specified in Table 1 and Table 2. The single row bolt arrangement of 11 bolts is subjected to 4-point loading, which have the roller and pinned support at each end and imposed by two-point load on top of the beam is shown in Figure1.

Table 1: The Dimension of the Lipped Channel Back-To-Back.

Lipped Channel (back-to-back)				
Nominal Dimensions (mm)				Section Area
Depth	Width	Lip	Thickness	(mm ²)
300	65	15	3	2576

Table 2: The Properties of the Lipped Channel Back-To-Back.

Mass (kg/m)	Second Moment of Area (10 ⁶ mm ⁴)		Section Modulus (10 ³ mm ³)		Reduced Properties (10 ³ mm ³)		Radius of Gyration (mm)	
Galv.	Ix	Iy	Zx	Zy	Zx red	Zy red	rx	ry
20.22	30.62	1.50	204.2	23.09	191.4	23.09	109.00	24.10

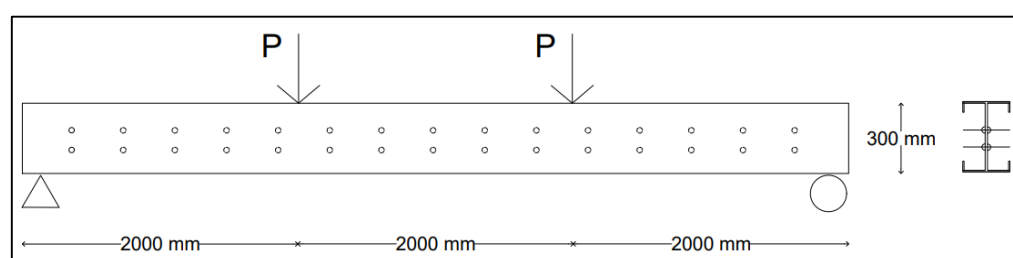


Figure 1: Schematic Diagram of CFS I-Beam.

2.2 Cold-Formed Steel I-Section Beam Series I

For this study, the cold- formed steel built-up I-section beam using back-to-back plain channel was developed for two different types of bolt arrangement as shown in Table 3 in order to investigate the effect of bolt arrangement on the structural behaviors. Table 4 and Table 5 show the dimension and properties of plain channel section.

Table 3: Bolt Notation of Finite Element Models.

Model ID	Type of Bolt Arrangement	Size of Bolt (mm)	Number of Bolt per Row	Rows of Bolts	Total Number of Bolt
S	Single row	12	11	1	11
D	Double rows			2	22

Table 4: The Dimension of Plain Channel Section Back-to-Back.

Plain Channel (back-to-back)				
Nominal Dimensions (mm)				Section Area
Depth	Width	Radius	Thickness	(mm ²)
152	102	3.2	3.0	1470

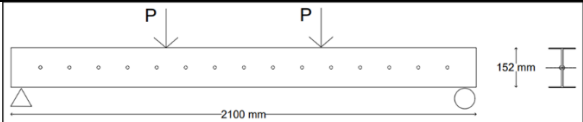
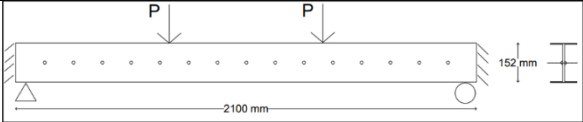
Table 5: The Properties of Plain Channel Section Back-to-Back.

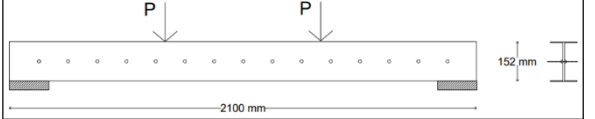
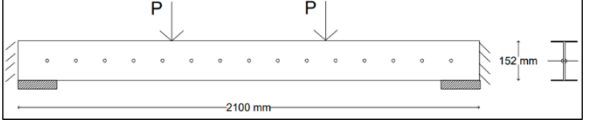
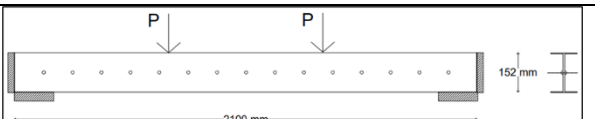
Mass (kg/m)	Second Moment of Area (10 ⁶ mm ⁴)		Section Modulus (10 ³ mm ³)		Reduced Properties (10 ³ mm ³)		Radius of Gyration (mm)	
Galv.	I _x	I _y	Z _x	Z _y	Z _{x red}	Z _{y red}	r _x	r _y
11.72	4.84	0.57	63.80	10.99	60.20	9.27	57.40	19.70

2.3 Cold-Formed Steel I-Section Beam Series II

The two types of beams that have been mentioned earlier in Series I are subjected to four-point loading in order to simulate the real support and loading condition., which is exposed to five support conditions as shown in Table 6 and imposed by two-point load (1kN concentrated load on top) at the distance of 700 mm from each end.

Table 6: Support Notation of Finite Element Models.

Model ID	Support Left	Support Right	Support Illustration
S1 & D1	Translation in X, Y, Z direction	Translation in Y direction	
S2 & D2	Translation in X, Y, Z direction & Lateral translation in Z direction	Translation in Y direction & Lateral translation in Z direction	

S3 & D3	Fixed support	Fixed support	
S4 & D4	Fixed support & Lateral translation in Z direction	Fixed support & Lateral translation in Z direction	
S5 & D5	Fixed support & Lateral fixed	Fixed support & Lateral fixed	

2.4 Finite Element System

In LUSAS finite element system, there are three main stages for the complete finite element analysis. The stages are including pre-processing, processing, and post-processing.

2.4.1 Pre-Processing

Pre-processing stage involves construct geometrical modelling which represents of the structure of cold-formed steel built-up I-section beam. This stage also involves assigning material properties, support, and loading condition.

2.4.2 Processing

When the modelling of structure is complete, the next stage is running the buckling analysis by eigenvalue. LUSAS will create the data file from the model generated. The outcome from finite element solver contains the required data needed.

2.4.3 Post-Processing

Post-processing or results processing is the visualization of the results produced from an analysis. Visualizing results is including deformed mesh and printed result.

2.5 Finite Element Modelling

The finite element model of the cold-formed steel I-beam section was represented by a 3D surface model and discretized by utilizing the thick shell element (QTS8) with the element size of 50 mm. Then the 3D joint features joining two points are used to model the bolted connections parts of the I-beam were discretized by utilizing as joint no rotational stiffness with one division (JNT4). Before the I-shaped model as shown in Figure 3 obtained, two different C-section need to be modelled separately as shown in Figure 2. Each type of bolt arrangement was modelled in 12mm size of bolt. The size of bolt is determined by insert the appropriate value of elastic spring stiffness which is 2108 kN/mm into the joint material attribute. In this study, the isotropic material property was used to specify the cold-formed steel's material properties. CFS beams with two different bolt arrangement are exposed to five different loading conditions and imposed by two-point load (1kN concentrated load on top) at the distance of 700mm from each end. The beams were analyzed by eigenvalue of buckling analysis. When the modelling process is complete, LUSAS Solver will create the results including the buckling mode of the structure and eigenvalue buckling load capacity result.

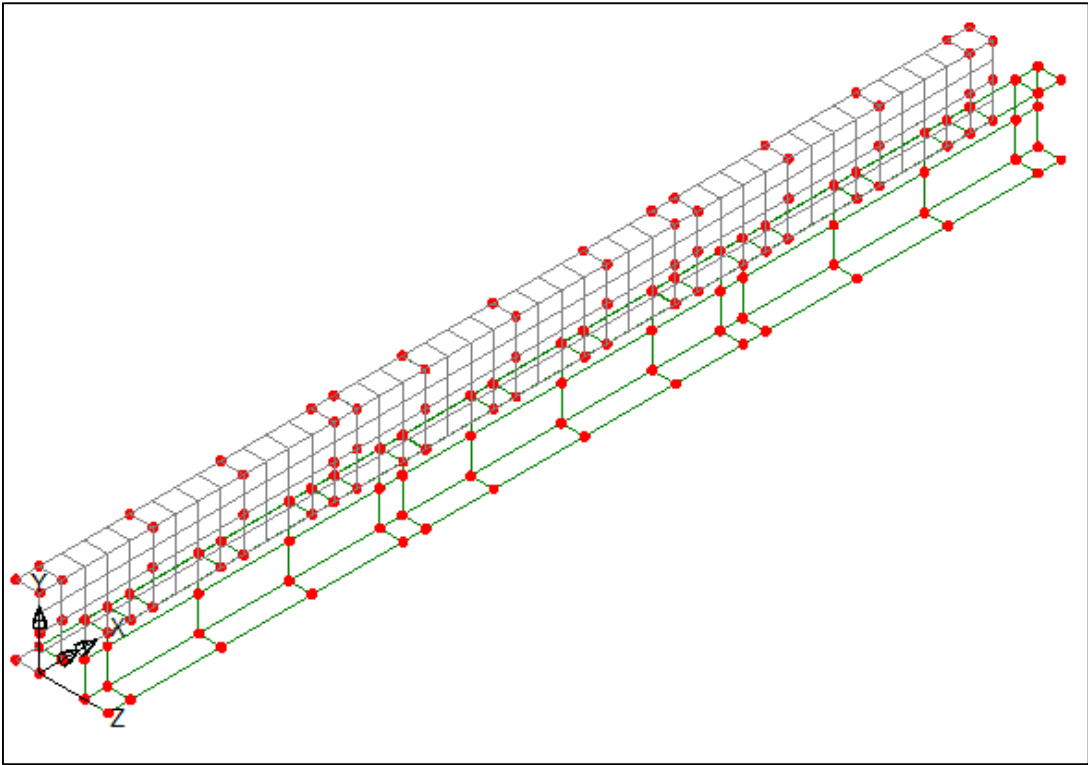


Figure 2: Modelling of two different C-section beam.

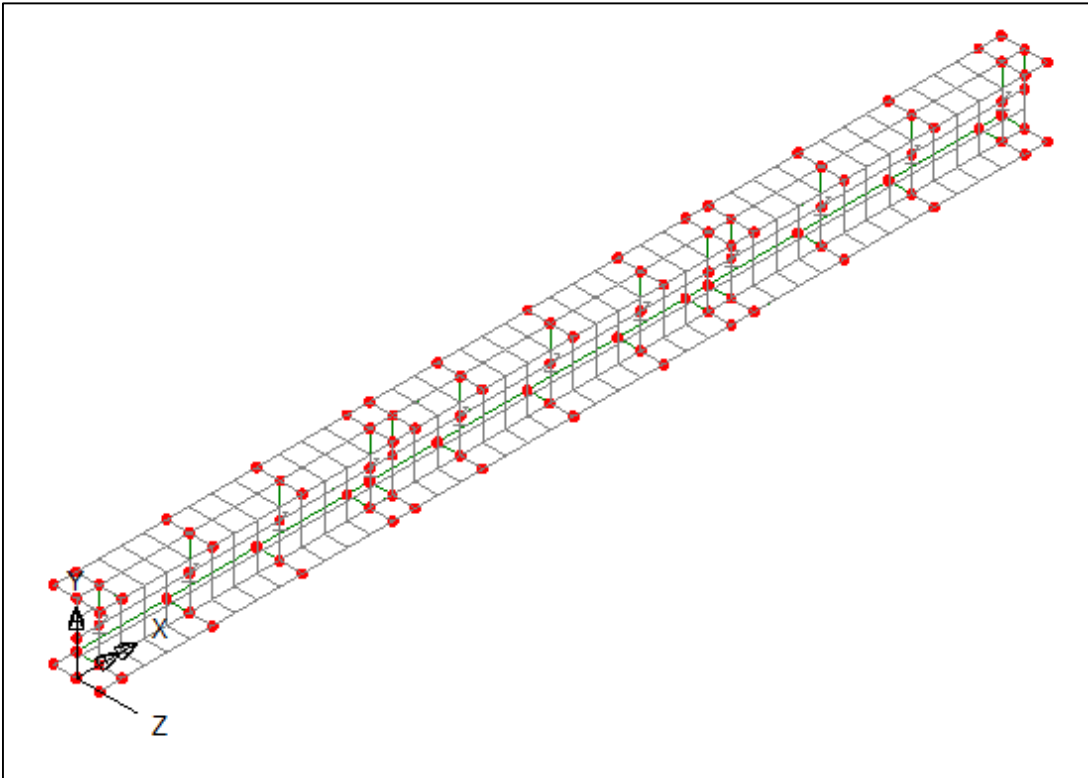


Figure 3: Model of cold-formed steel I-beam.

3. Results and Discussion

The results of the analysis are presented in form of deformed mesh plots and table as summary for the result obtained. Therefore, some comparisons were made by observed the obtained results according to the models with different parameters.

3.1 Validation of Finite Element Analysis

Table 7 shows the validation of results between theoretical value, finite element analysis and previous finite element analysis by Wong (2006). The buckling load obtained from LUSAS finite element analysis is same with the theoretical value. Figure 4 shows the buckling mode of the cold formed-steel built-up I-section beams when reached its buckling load capacity. As the result shows, the beam tends to twist to either side. Therefore, buckling mode was similar with the previous study. Wong (2006) stated that the I-beam fails in the mode of lateral torsional buckling. The beam tends to displace laterally and twisting to either side. Hence, the beam also bent about its major axis. The mid-span had larger lateral displacement compared to the end of the beam. This restraint also causes the top flange of the beam buckle or twist to either side.

Table 7: Validation of the Result.

Theoretical	Buckling Load (kN)	
	Previous FEA	LUSAS FEA
7.56	4.49	7.56

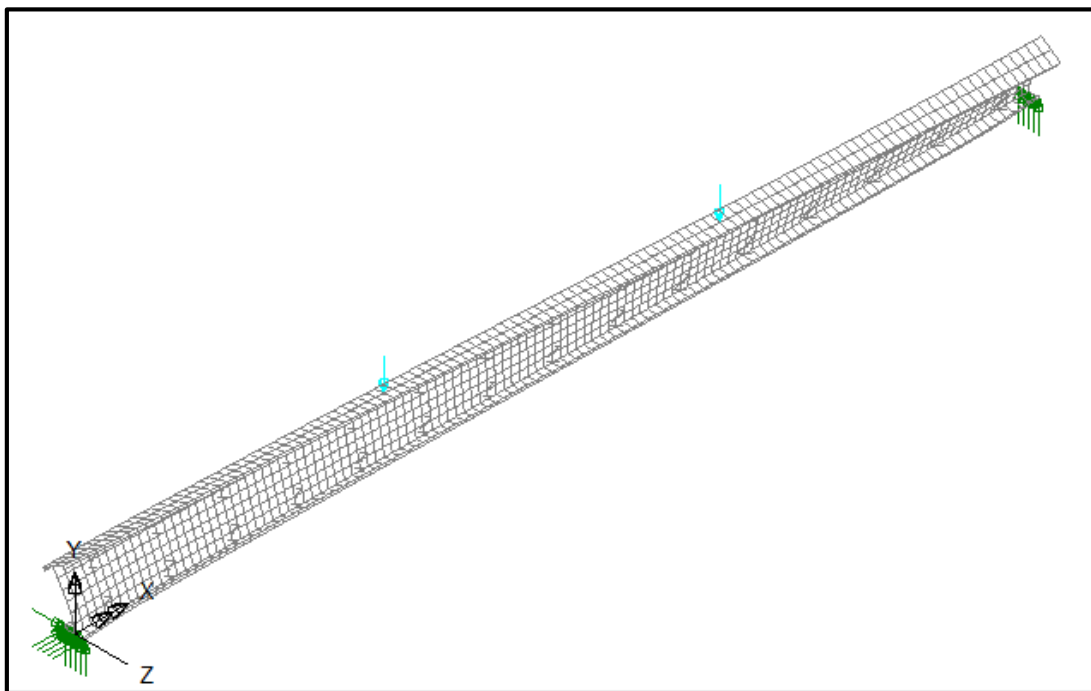


Figure 4: Buckling mode of control built-up I-beam

3.2 FEA Result of Cold-Formed Steel Built-Up I-Section Beam

3.2.1 Buckling Load Capacity

Table 8 shows the buckling load capacity of single and double row bolt arrangement of cold-formed steel built-up I-section beams. The percentage different between single and double row bolt arrangement are summarized in the table.

Table 8: Buckling Load Capacity

Single Row Bolt Arrangement		Double Row Bolt Arrangement		Percentage Different (%)
Model ID	Buckling Load (kN)	Model ID	Buckling Load (kN)	
S1	12.63	D1	15.76	24.78
S2	23.00	D2	56.28	144.70
S3	20.17	D3	19.61	-2.77
S4	30.70	D4	59.54	93.94
S5	38.81	D5	88.42	127.83

3.2.2 Buckling Mode

The buckling mode of FEA models of cold-formed steel built-up I-section beams are shown in Appendix A. From the FEA, single and double rows of cold-formed built-up I-section performed almost the same buckling behavior. The beams are failed in the mode of lateral torsional buckling. The beam tends to displace laterally and twisting to either side.

3.3 Comparison of Parametric Study

3.3.1 Effect of Bolt Arrangements on Buckling Load

From the result obtained in Figure 5, the results show the logical expectation with the increasing number of bolts which induce the buckling capacity of cold-formed steel beam. However, the buckling load capacity of model S3 and D3 did not increase dramatically when number of bolts are added. So, from the result, it clearly shows that the effect of bolt arrangement of the built-up I-beam on buckling load is truly significant.

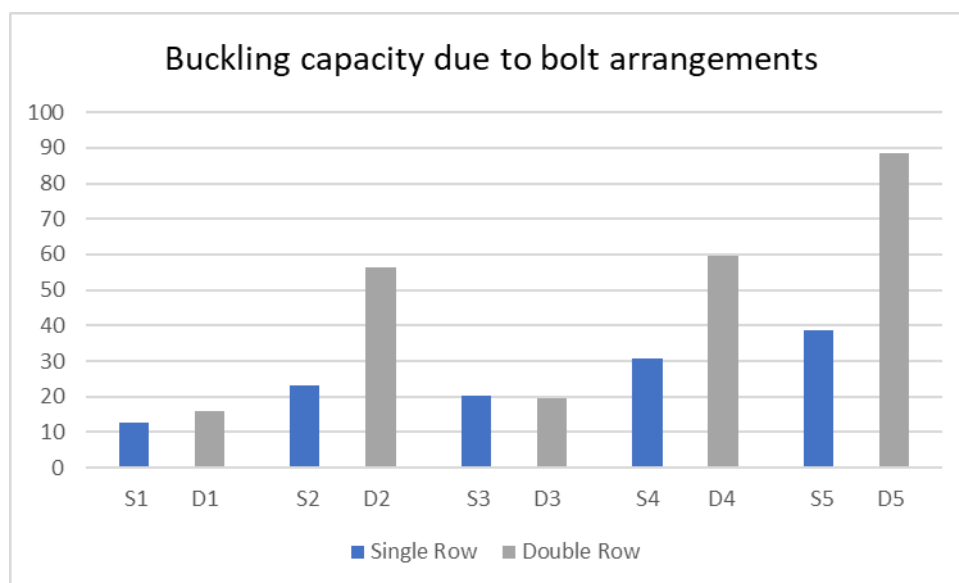


Figure 5: Buckling load capacity due to bolt arrangements.

3.3.2 Effect of End-Restraint Support on Buckling Load and Buckling Mode

Figure 6 and Figure 7 show the comparison with single row and double row bolt arrangement of cold-formed I-beams, it clearly shows that the change of support of cold-formed steel built-up I-beam has significant effect on the buckling load and buckling mode of the beam. From this case, cold-formed steel beam that have the lateral end-restraint support gained higher buckling load capacity. Moreover, deformed pattern of lateral end-restraint beam minimizes the twisting of the beam. Thus, it clearly shows beams with lateral end-restraint stronger compared to simply supported beam. End-restraint support also can prevent twisting of the cold-formed steel beams.

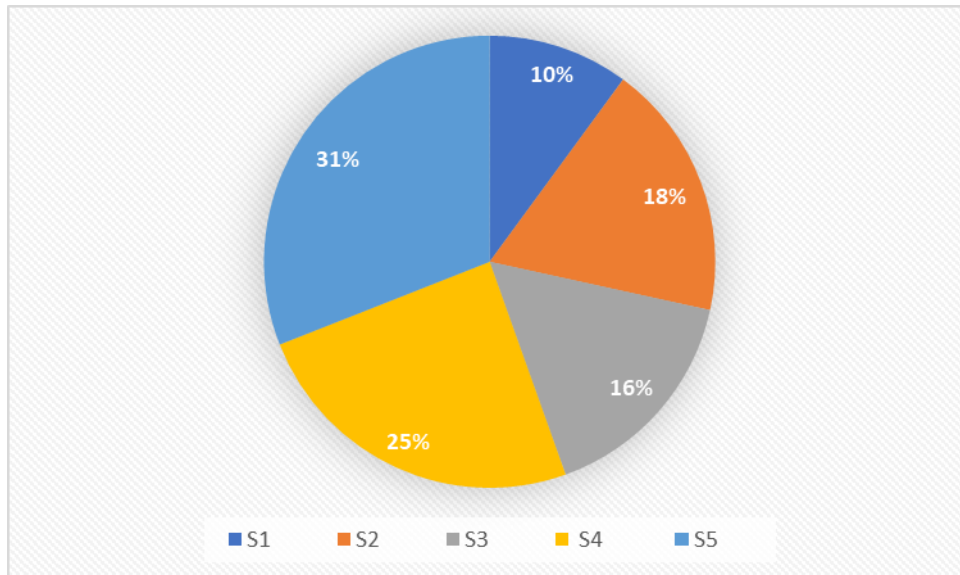


Figure 6: Comparison of buckling capacity within single row I-beams.

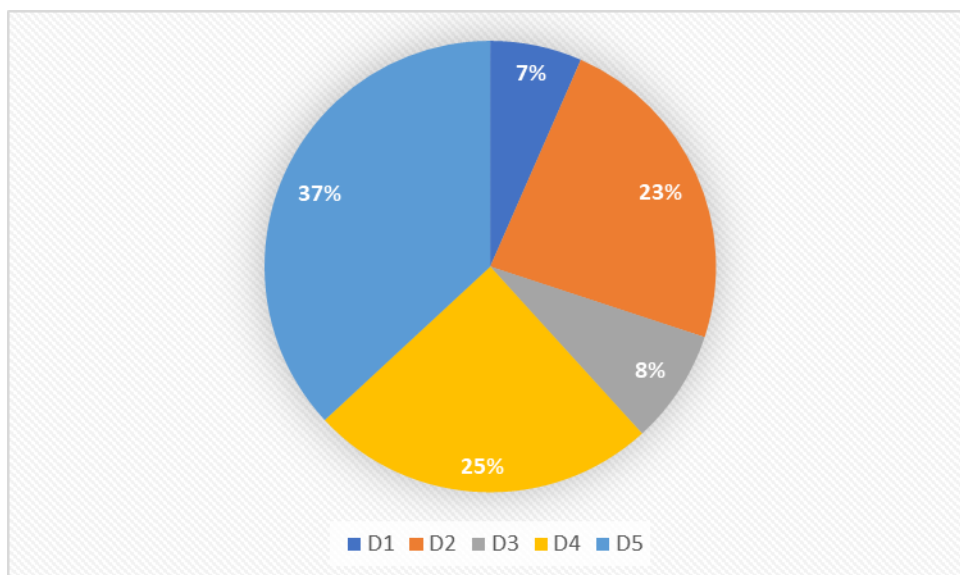


Figure 7: Comparison of buckling capacity within double row I-beams.

4. Conclusion

The study shows that the finite element method is a useful research tool for studying the structural behavior of cold-formed steel structures. The objective of this project is to determine the buckling load of cold-formed steel built-up I section beams and investigate the effect of end-restraint and the bolts arrangements towards the buckling load of cold-formed steel built-up I-section beams based on computational study. The total of 10 models of cold-formed steel beams are modelled using finite element method by LUSAS finite element software. There are 2 types of bolt arrangement which is single row and double row bolt arrangement that subjected to four-point loading, which is exposed to five different end-support conditions and imposed by two-point load. Based on the FEA outcome, the result achieved the logical expectation with the increasing number of bolts which induce the buckling capacity of cold-formed steel beam. Moreover, the beams with lateral end-restraint support achieved higher buckling load capacity and have the minimum twisting effect of the deformed pattern of the beams. The bolt arrangement and the type of end-support are greatly affecting the performance of cold-formed steel built-up I-section beams.

References

- [1] K. Roy, H. Ho Lau, T. C. H. Ting, B. Chen, and J. B. P. Lim, "Flexural behaviour of back-to-back built-up cold-formed steel channel beams: Experiments and finite element modelling," *Structures*, vol. 29, no. December 2020, pp. 235–253, 2021, doi: 10.1016/j.istruc.2020.10.052.
- [2] K. J. R. Rasmussen, M. Khezri, B. W. Schafer, and H. Zhang, "The mechanics of built-up cold-formed steel members," *Thin-Walled Struct.*, vol. 154, p. 106756, 2020, doi: 10.1016/j.tws.2020.106756.
- [3] S. M. Mojtabaei, I. Hajirasouliha, and J. Ye, "Optimisation of cold-formed steel beams for best seismic performance in bolted moment connections," *J. Constr. Steel Res.*, vol. 181, p. 106621, 2021, doi: 10.1016/j.jcsr.2021.106621.
- [4] S. Selvaraj and M. Madhavan, "Design of Cold-Formed Steel Back-To-Back Connected Built-up Beams," *J. Constr. Steel Res.*, vol. 181, p. 106623, 2021, doi: 10.1016/j.jcsr.2021.106623.
- [5] K. V. Satheesh Kumar, P. Selvakumar, R. Jagadeeswari, M. Dharmaraj, K. R. Uvanshankar, and B. Yogeswaran, "Stress analysis of riveted and bolted joints using analytical and experimental approach," *Mater. Today Proc.*, vol. 42, pp. 1091–1099, 2020, doi: 10.1016/j.matpr.2020.12.268.
- [6] J. H. Zhang and B. Young, "Finite element analysis and design of cold-formed steel built-up closed section columns with web stiffeners," *Thin-Walled Struct.*, vol. 131, no. June, pp. 223–237, 2018, doi: 10.1016/j.tws.2018.06.008.

Appendix A

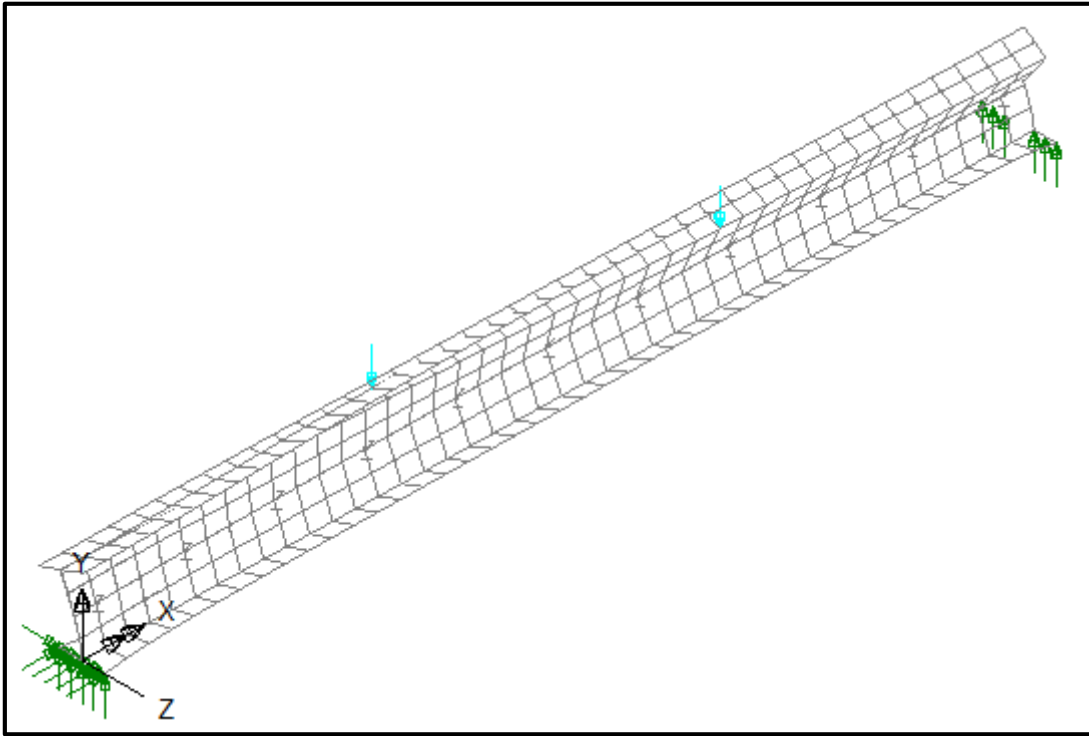


Figure A.1: The buckling mode of S1 beam.

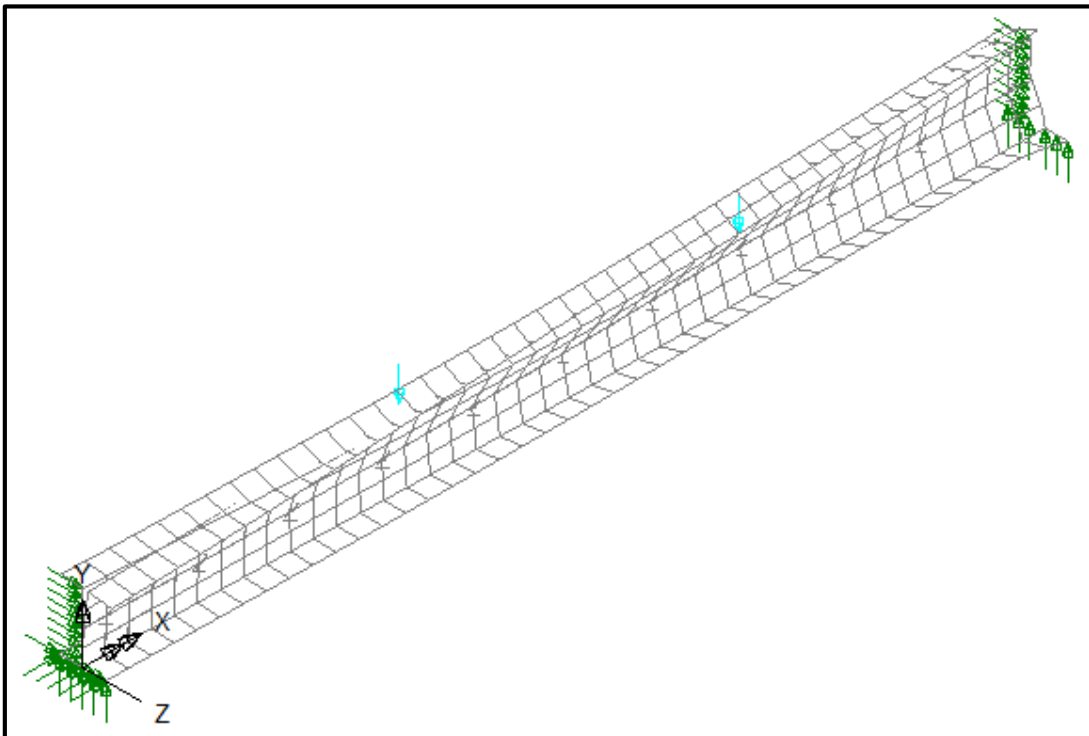


Figure A.2: The buckling mode of S2 beam.

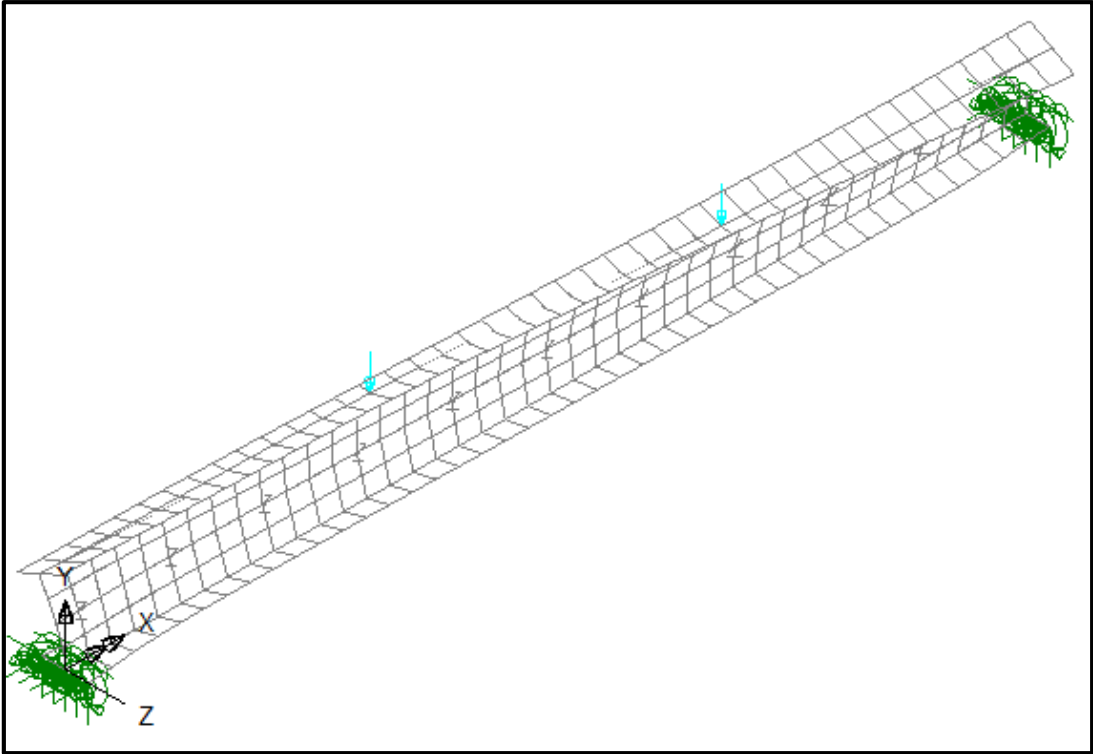


Figure A.3: The buckling mode of S3 beam.

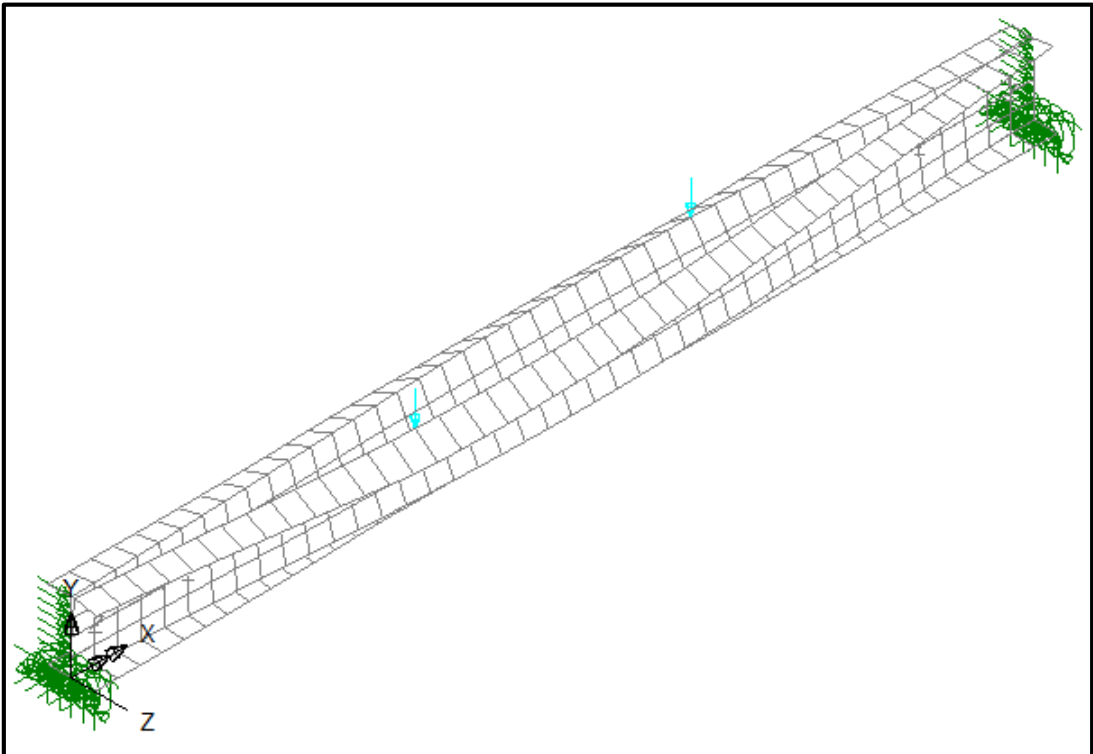


Figure A.4: The buckling mode of S4 beam.

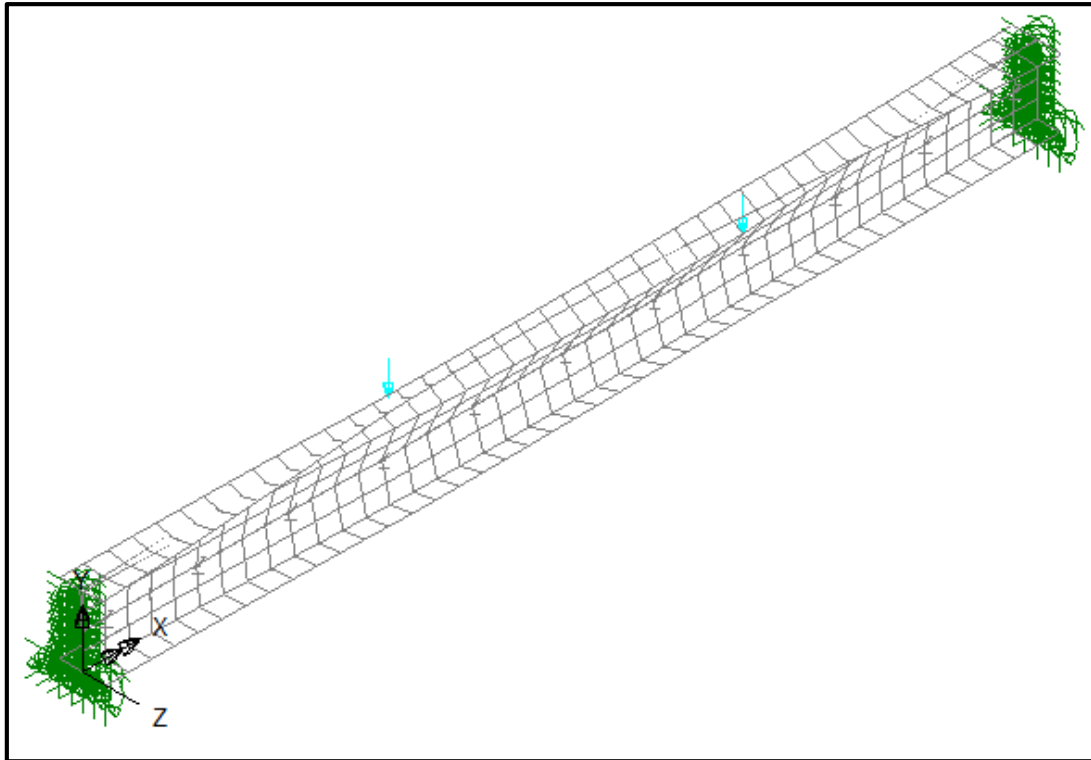


Figure A.5: The buckling mode of S5 beam.

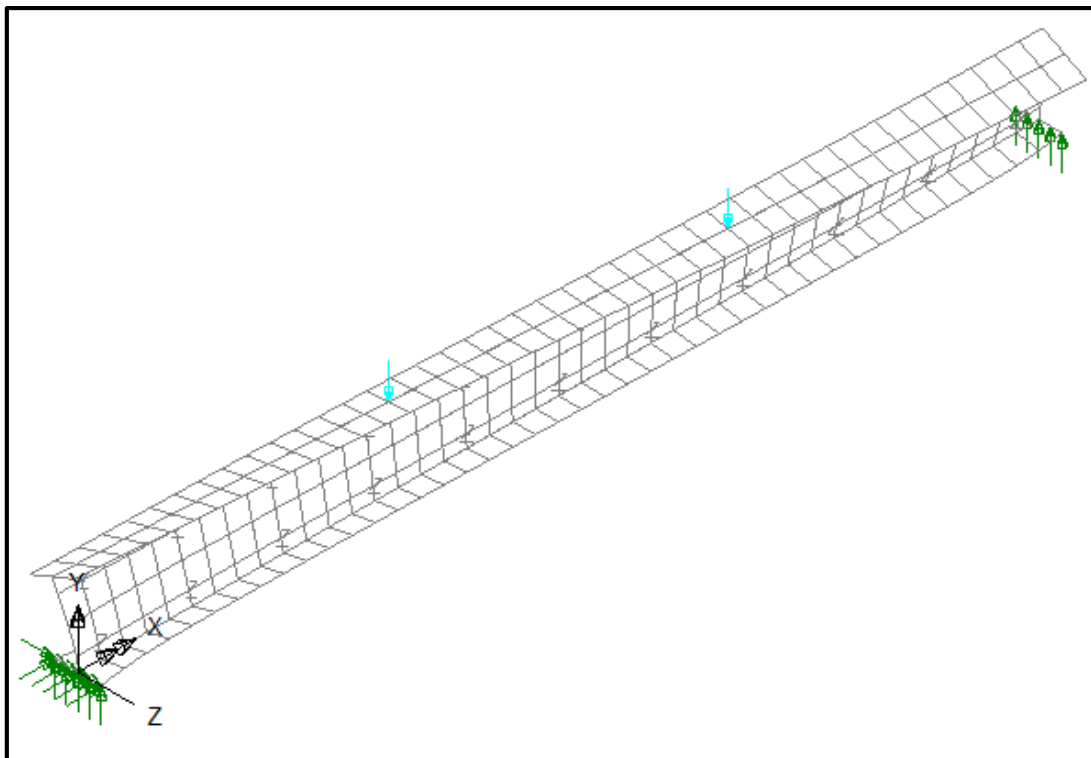


Figure A.6: The buckling mode of D1 beam.

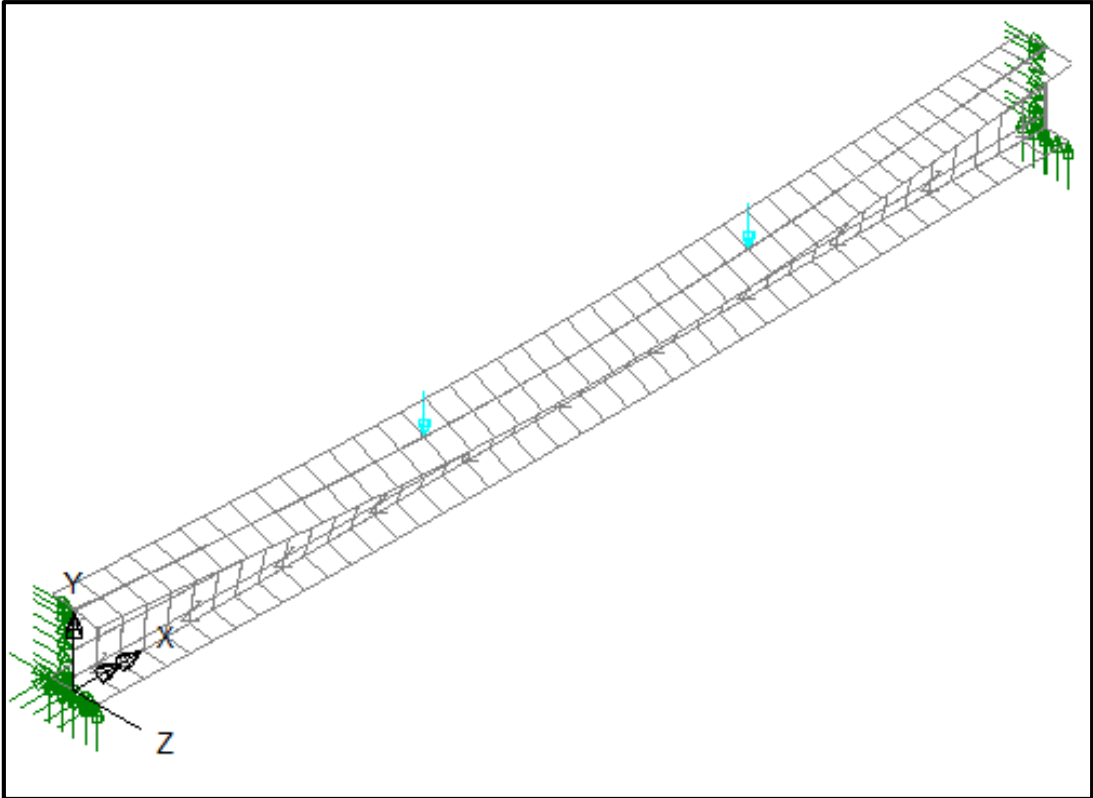


Figure A.7: The buckling mode of D2 beam.

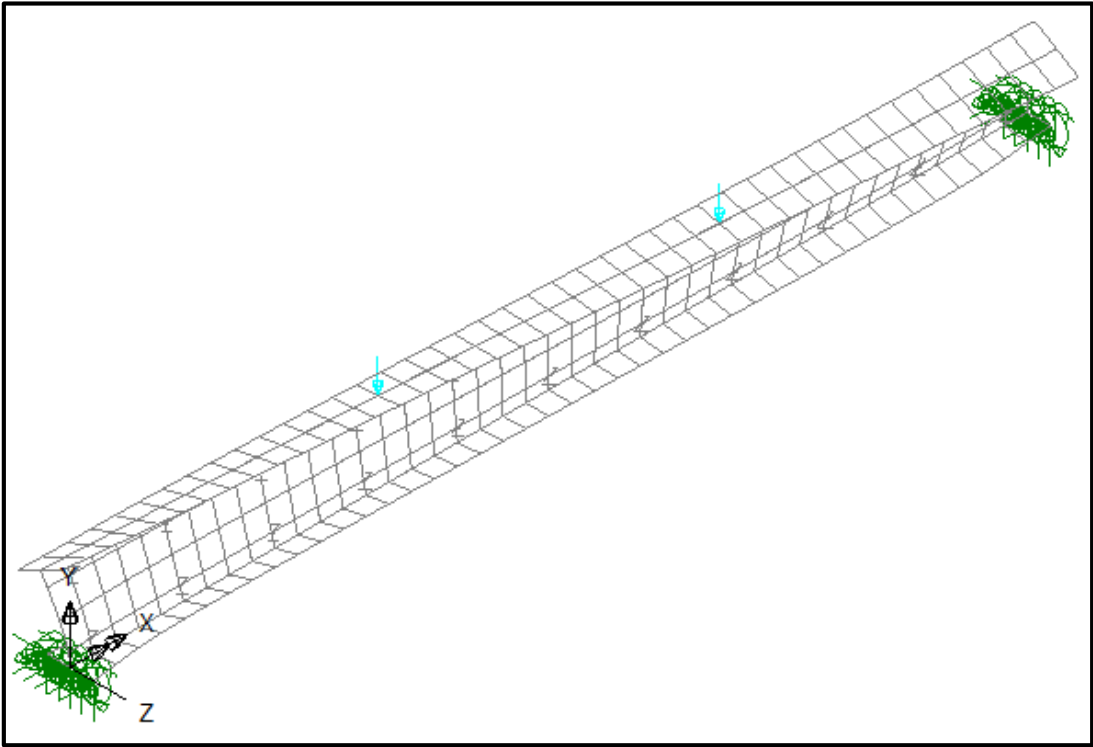


Figure A.8: The buckling mode of D3 beam.

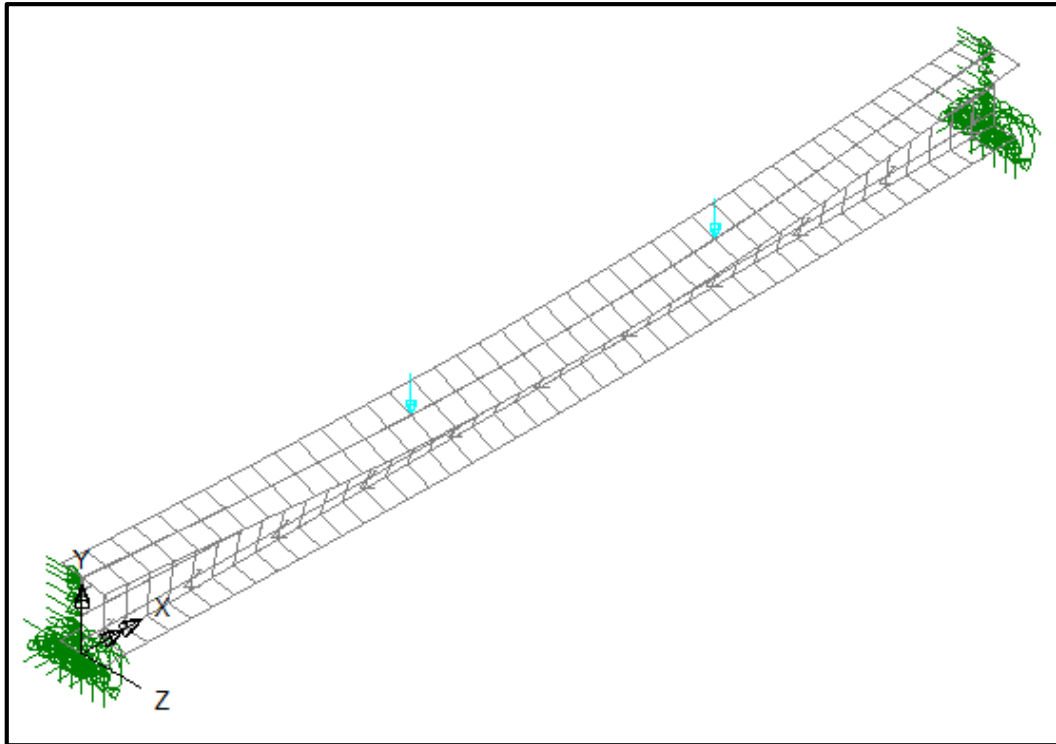


Figure A.9: The buckling mode of D4 beam.

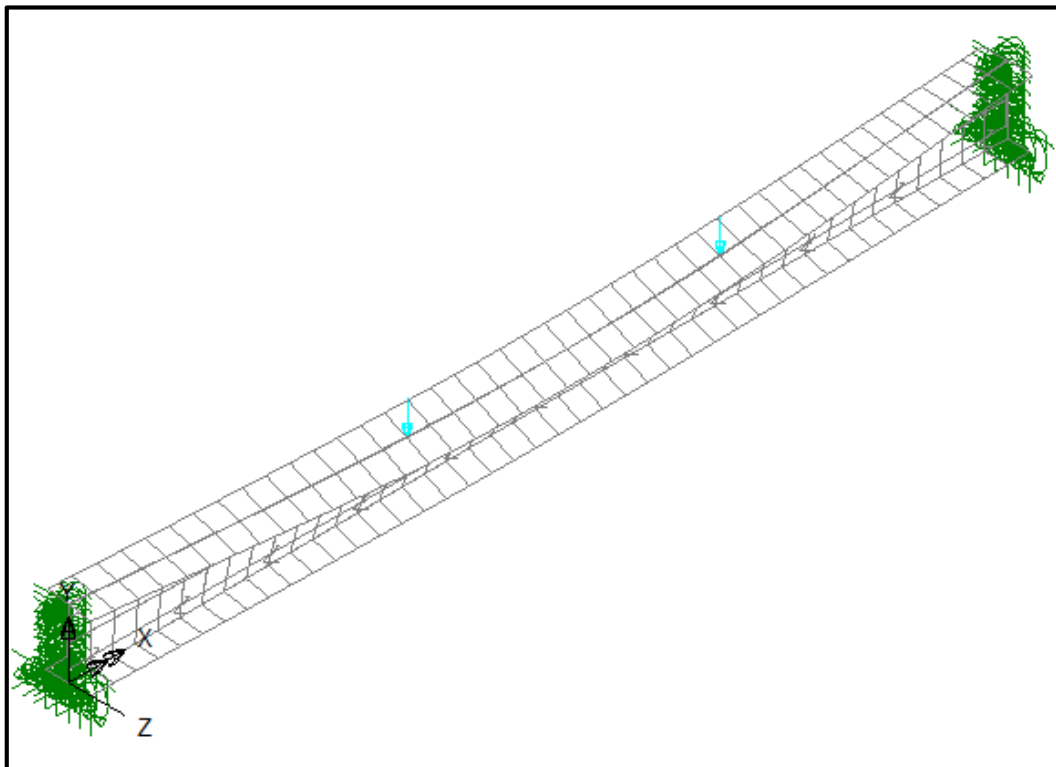


Figure A.10: The buckling mode of D5 beam.